IAES International Journal of Artificial Intelligence (IJ-AI)
Vol. 15, No. 4, August 2026, pp. 3120~3130
ISSN: 2252-8938, DOI: 10.11591/ijai.v15.i4.pp3120-3130

Deep learning for lung cancer diagnosis: a comparative artificial intelligence study

Phaneendra Varma Chintalapati[1], Prasanth Aruchamy[1], Alur Praneetha[2]
[1]Department of Computer Science and Engineering, Vel Tech Rangarajan Dr. Sagunthala R&D Institute of Science and Technology, Chennai, India
[2]Department of Computer Science and Engineering, Koneru Lakshmaiah Education Foundation, Vaddeswaram, India

Article Info

Article history:

Received Sep 11, 2025
Revised May 20, 2026
Accepted Jun 19, 2026

Keywords:

AI-driven diagnostics
Convolutional neural networks
Deep learning
Lung cancer detection
Residual network

ABSTRACT

Early and accurate lung cancer diagnosis (LCD) is critical, yet traditional imaging methods such as X-rays and computed tomography (CT) scans are costly, invasive, and heavily reliant on expert interpretation. This study investigates artificial intelligence (AI)-driven diagnostics by comparing deep learning models (convolutional neural network (CNN), residual network (ResNet), and visual geometry group 16 (VGG16)) with traditional machine learning algorithms (logistic regression (LR) and support vector machine (SVM)), using lung image database consortium and image database resource initiative (LIDC-IDRI) and Kaggle lung CT scan datasets. Performance was evaluated across multiple metrics: accuracy, sensitivity, specificity, and area under the curve-receiver operating characteristic (AUC-ROC). Among the models, ResNet achieved the highest performance, with an accuracy of 94%, sensitivity of 95%, specificity of 93%, and AUC-ROC close to 1. CNN and VGG16 also showed superior metrics compared to LR and SVM, highlighting the robustness of deep learning techniques. These results demonstrate that deep learning models not only achieve higher diagnostic accuracy but also significantly reduce false detections compared to traditional approaches. The findings support the potential of AI to automate and enhance LCD, thereby improving accessibility, consistency, and speed in clinical settings. Future work will emphasize clinical validation, address ethical challenges, and focus on integrating AI models into real-world healthcare workflows to improve patient outcomes.

Corresponding Author:

Phaneendra Varma Chintalapati
Department of Computer Science and Engineering
Vel Tech Rangarajan Dr. Sagunthala R&D Institute of Science and Technology
Avadi, Chennai, India
Email: vtd1106@veltech.edu.in

1. INTRODUCTION

Nearly 18% of global cancer fatalities are due to lung cancer. Accurate diagnosis is crucial for early interventions to enhance patient survival. Computed tomography (CT) scans and chest X-rays are utilized, but they are invasive, expensive, and require professional knowledge, limiting their availability and efficacy [1]. Recent advances, particularly deep learning-based ones, have made lung cancer diagnosis (LCD) non-invasive, cost-effective, and efficient [2]. Deep learning models, especially convolutional neural networks (CNNs), have demonstrated remarkable capabilities in medical image analysis, offering potential for improved sensitivity, specificity, and efficiency in lung cancer detection and classification [1], [3], [4].

CNNs can identify and categorize malignant tumors in medical imaging datasets. These developments increase diagnostic accuracy and enable seamless integration of automated technology into clinical workflows, making early detection easier and more reliable [5]. Previous diagnostic approaches are compared to deep learning methods to explain how they might overcome their disadvantages. By comparing these methods, the potential of deep learning to enhance lung cancer detection and outcomes can be understood [6].

Recent research shows deep learning systems may detect lung cancer. Deep learning algorithms can automatically classify lung cancer in X-rays, whole slide images (WSI), CT scans, and magnetic resonance imaging (MRI), according to comprehensive research. Another study found that deep learning algorithms can enhance positron emission tomography (PET)/CT lung cancer detection for early diagnosis and tailored treatment [7].

Deep learning allows models to diagnose and categorize lung cancers independently using histopathology pictures. This study revealed that deep learning could be used to diagnose malignancies and predict patient outcomes based on histological markers. Deep learning may enhance LCD and detection [8]. Deep learning technology is intriguing, but clinical use presents challenges that can be overcome [9]. Ethics, validation across several patient populations, and fair access to artificial intelligence (AI)-powered diagnostic technologies are important challenges. Deep learning algorithms for LCD were evaluated and shown to need additional study to solve these challenges and boost AI-based clinical diagnostics [10]. Deep learning may identify lung cancer. Deep learning algorithms can improve healthcare, diagnosis accuracy, and patient outcomes by predicting diagnostic constraints [11]. Future research must overcome current obstacles to bring new technology into clinical practice.

By comparing the performance of different deep learning models, this comparative study aims to provide a comprehensive overview of the current state-of-the-art in AI-assisted LCD. It also examines their strengths and weaknesses. This exploration will contribute to the ongoing efforts to improve early detection, personalize treatment strategies, and ultimately enhance the survival rates of individuals affected by this devastating disease [12].

Research has demonstrated the efficacy and therapeutic promise of deep learning approaches for lung cancer screening. A comprehensive analysis by Javed *et al.* [1] highlighted the usefulness of deep convolutional neural networks (DCNNs) in automating lung cancer detection using X-rays, WSI, CT scans, and MRI. Bouchaffra *et al.* [13] used deep learning in low-dose CT screening programs to identify and stratify lung cancer in high-risk populations. Deep learning has improved histopathological analysis, with Kalkan *et al.* [14] showing automated lung tissue tumor identification and characterization for accurate diagnosis and prognosis. In a thorough assessment of deep learning models for early-stage lung cancer detection, Hosseini *et al*. [2] identified problems and potential approaches.

LCD using CT images has been significantly enhanced through deep learning techniques. Mamun *et al.* [15] proposed the LCDctCNN, demonstrating high accuracy and recall for LCD. Liu *et al.* [16] reviewed the evolution of pulmonary nodule detection over the past three decades, highlighting the transition from conventional image analysis to deep learning-based decision support. Wang [17] comprehensively discussed recent deep learning techniques for LCD, emphasizing their potential to improve diagnostic accuracy, early detection, and clinical decision-making. Sohn and Fields [18] demonstrated that the integration of radiomics and deep learning enables accurate prediction of pulmonary nodule metastasis from CT images, thereby supporting precision medicine. Hashimoto *et al*. [19] highlighted the opportunities and challenges of AI in healthcare, emphasizing its potential to improve diagnostic efficiency and clinical outcomes. Lee *et al.* [20] reviewed the current status and future directions of radiomics in lung cancer, demonstrating its role in extracting quantitative imaging biomarkers for diagnosis and prognosis. Furthermore, Zhang *et al.* [21] performed a systematic review and meta-analysis, confirming the high diagnostic performance of CNNs in pulmonary nodule detection and reinforcing their effectiveness in computer-aided LCD.

Deep learning has been used with genomes and clinical data to enhance lung cancer detection algorithms. Transfer learning has also been used to identify lung cancer using pre-trained models without big annotated datasets. Explainable artificial intelligence (XAI) models are emphasized in deep learning-based lung cancer detection systems to provide transparency and trustworthiness. For faster decision-making and better patient outcomes, clinical deep-learning models have been tested in real time.

2. CHALLENGES AND UNADDRESSED ISSUES

Classic and modern lung cancer screening methods remain understudied despite medical imaging and AI breakthroughs. Chest X-rays, CT scans, and biopsies are commonly used, but their invasiveness, high cost, and reliance on expert interpretation limit their use, especially in resource-constrained countries. Deep learning approaches like CNNs, residual network (ResNet), and visual geometry group 16 (VGG16)

enhance accuracy and efficiency without surgery. Early studies seldom compare these algorithms' performance on many real-world datasets. Clinical accuracy, sensitivity, and scalability are rarely addressed. This discrepancy highlights the necessity to integrate old and modern approaches fully. These issues are addressed via a rigorous study that compares existing diagnostic methods to deep learning-based lung cancer detection models. For accuracy, sensitivity, and scalability, CNNs, ResNet, and VGG16 will be tested on lung image database consortium and image database resource initiative (LIDC-IDRI) and Kaggle lung cancer datasets is illustrated in Table 1.

Table 1. Comparative analysis of deep learning algorithms for lung cancer detection

Reference	Algorithm	Extracted features	Accuracy performance
Javed *et al.* [1]	DCNNs	Automated feature extraction from X-rays, WSI, CT scans, and MRI	High accuracy across multiple imaging modalities
Mamun *et al.* [15]	LCDctCNN	Features from CT scan images	Accuracy: 92%
Zhang *et al*. [21]	CNN	Hierarchical features automatically extracted from pulmonary CT images	High diagnostic accuracy for pulmonary nodule detection based on systematic review and meta-analysis.
Suzuki [22]	Massive training artificial neural network (MTANN)	Features from low-dose CT scans	Reduction of false positives in nodule detection
Vázquez *et al.* [23]	CNN for mammographic microcalcifications	Pattern recognition features from mammograms	Achieved up to 89.56% accuracy
Mittal *et al.* [24]	Neural network for liver lesion classification	Features of CT focal liver lesions	Improved classification accuracy
Varma *et al.* [25]	CNN for carotid atherosclerosis diagnosis	Ultrasound image statistics and texture features	Enhanced diagnostic accuracy
Orozco *et al.* [26]	Support vector classification for lung nodule detection	Features from chest radiographs	Improved detection accuracy

Each strategy's pros and cons will highlight AI-driven diagnostics' transformative potential while addressing scalability and clinical integration issues. Finally, this initiative will develop and implement therapies to enhance early LCD to advance the field. Deep learning has significantly advanced lung cancer detection across imaging modalities like CT, MRI, and histopathology; nevertheless, several critical research gaps remain. Most studies, including those by authors [1], [2], highlight limitations such as data heterogeneity, lack of standardized imaging protocols, and challenges in generalizing models across diverse populations. There is a shortage of large, annotated datasets needed for robust model training, as discussed by Liu *et al.* [16].

Moreover, although XAI and real-time clinical deployment have been explored, building fully transparent, bias-free, and ethically sound AI systems still requires more focused research. Integration of multimodal data (imaging, clinical, and molecular) for comprehensive diagnosis and personalized therapy remains underdeveloped. Further, validation studies in real-world clinical environments are limited, and ensuring equity and fairness across different demographic groups in AI-driven lung cancer diagnostics is a major future need.

3. METHOD

3.1. Data collection

The LIDC-IDRI collection comprises radiologists' nodules categorized in lung CT images, which includes demographics and clinical history. The Kaggle dataset shows lung CT images with or without cancer. In model construction, standard machine learning and modern deep learning models are used and trained. Each solution has advantages and meets design goals. Logistic regression (LR) and support vector machine (SVM) are fundamental models. Preprocessing provides human-defined lung nodule size, shape, and texture for these algorithms. Although computationally efficient and interpretable, these models struggle with medical imaging's complex patterns.

This study analyzes clinically employed diagnostic methods such as chest X-rays, CT scans, and biopsies, which are invasive, costly, and need expert interpretation. Recently developed deep learning algorithms, such as CNNs, ResNet, and VGG16, offer automated, non-invasive, and efficient diagnostic solutions. Accuracy, sensitivity, and scalability are employed to assess the advantages and disadvantages of the approach, while robustness and real-world relevance are ensured through validation on benchmark datasets such as LIDC-IDRI and the Kaggle lung cancer dataset. This study aims to elucidate how novel

methodologies surpass traditional ones by examining performance disparities and identifying optimal clinical algorithms for the early identification and diagnosis of lung cancer. This study employs a four-stage framework: data collection, pre-processing, model development, and performance evaluation. This framework ensures robustness, reproducibility, and scalability for LCD.

The workflow framework of this study is presented in Figure 1, providing a clear and structured representation of the complete experimental and simulation pipeline to ensure reproducibility. Figure 1 illustrates data acquisition, preprocessing, model development, performance evaluation, and optimal model selection for LCD. At the outset, CT images were obtained from the LIDC-IDRI dataset with expert annotations and supplemented with clinical data from the Kaggle lung cancer dataset. The data were organized and split into training, validation, and testing sets to ensure unbiased evaluation. The data pre-processing stage includes a pre-processing [27], which includes contrast enhancement, histogram equalization, Gaussian, and median filtering for noise removal, and pixel normalization to standardize inputs across datasets. The datasets were systematically curated and integrated to ensure sufficient diversity and robustness for model development. The consolidated dataset was subsequently partitioned into three subsets, comprising 70% for training, 15% for validation, and 15% for testing. This stratified division facilitates effective model learning, enables hyperparameter tuning through validation, and ensures an unbiased evaluation of model performance on unseen data, thereby minimizing the risk of overfitting and enhancing generalization capability.

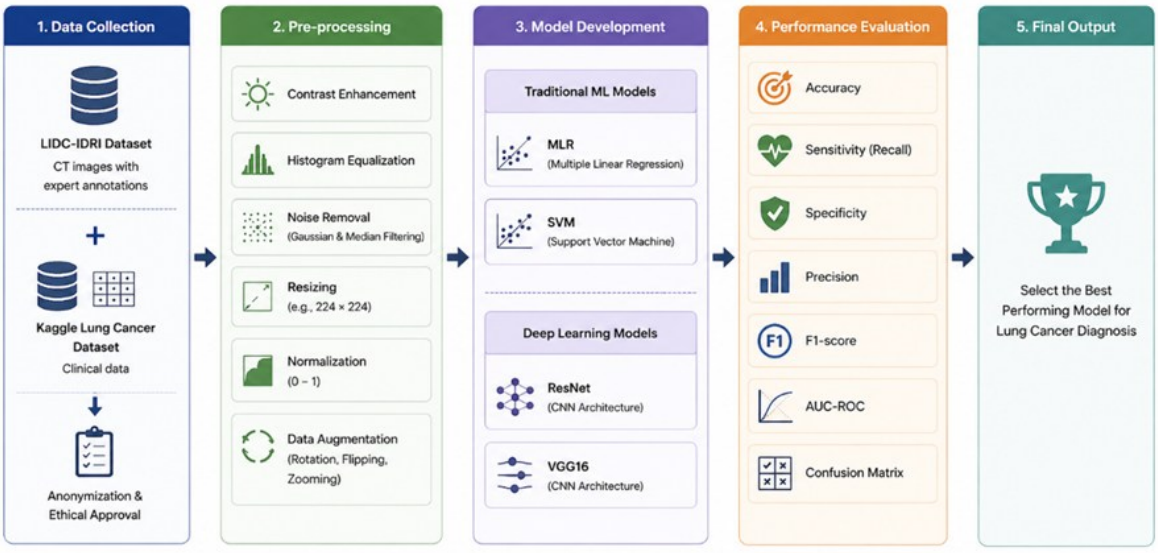

Figure 1. Comprehensive workflow of the proposed experimental and simulation workflow

In a broader sense, in medical images (e.g., CT scans), pixel values can vary widely due to differences in scanners, acquisition settings, or patient conditions. Pixel scaling normalization transforms these values into a fixed range- commonly [0, 1] or [-1, 1], using a linear scaling operation [28]. This helps stabilize training improves convergence of machine learning and deep learning models. By doing this, it is once again reiterated that pixel intensity normalization was performed by linearly scaling image values to the range [0, 1] to ensure uniform input distribution across datasets.

In the model development stage, both traditional machine learning models (LR and SVM) and deep learning models (CNNs with ResNet and VGG16 architectures) were developed. Deep models were trained using backpropagation with stochastic gradient descent, with hyperparameters optimized via validation. Finally, models were evaluated using accuracy, sensitivity, specificity, F1-score, and area under the curve-receiver operating characteristic (AUC-ROC), enabling a fair comparison of diagnostic performance and clinical reliability. The workflow follows a logical progression from data acquisition to final model selection, with clear interconnections between stages, ensuring transparency and ease of replication. The integration of this visual representation with the detailed methodological description provides a comprehensive and reproducible experimental framework for LCD.

3.2. Architecture diagram for lung cancer detection

The design emphasizes data collected from reliable sources, utilizing datasets from LIDC-IDRI and Kaggle. Figure 2 shows lung CT imaging data flow from collection to model deployment. The annotated lung CT scans from skilled radiologists are in LIDC-IDRI. It incorporates important metadata such as patient demographics, clinical history, and nodule characteristics for model development. The Kaggle dataset contains cancer-annotated lung CT images. The dataset is useful for creating and testing diagnostic algorithms. Data is organized and kept in a database or data lake for analysis after gathering. Data must be well-organized for development, usability, and traceability. Raw data must be preprocessed for model input to ensure consistency and picture quality. This phase uses multiple methods to highlight lung nodules and reduce artifacts, which include:

i) Image enhancement: histogram equalization and contrast modification help identify lung nodules. Enhanced photos help the model focus on key traits, improving diagnosis accuracy.
ii) Noise reduction: gaussian and median filters reduce CT image noise while preserving edges and texturing. This ensures noise does not impede the model's ability to detect meaningful patterns.
iii) Normalization: all photos are normalized to ensure pixel values are within a range, such as 0 to 1. Uniformly scaling input data speeds up and stabilizes model training convergence. These preparation methods provide data quality for feature extraction and model training, enabling accurate predictions.

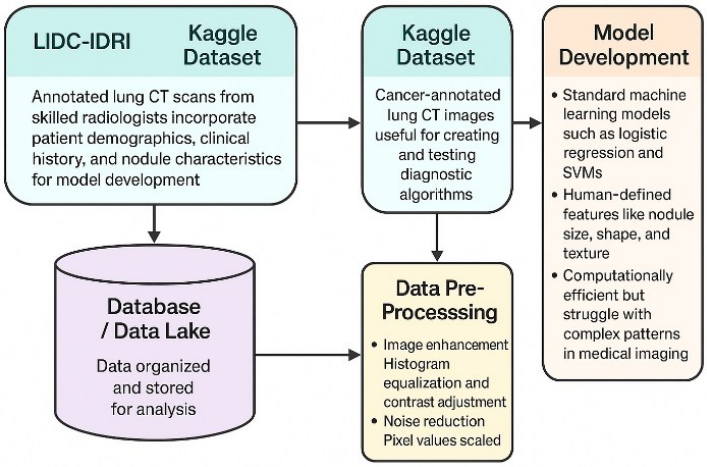

Figure 2. Lung CT imaging data flow: from collection to model deployment

3.3. Model development

Feature extraction is crucial to the detection of lung cancer because it transforms raw medical imaging data into meaningful numerical representations that can be analyzed by machine learning and deep learning algorithms. While older approaches need human feature engineering based on domain expertise, modern deep learning systems automatically identify features from the data. This paper provides a detailed explanation of the feature extraction processes and related mathematical formulas.

3.2.1. Logistic regression feature extraction

LR predicts the probability of outcome $P(Y = 1 \mid X)$ based on input characteristics in binary classification [28]. The probability of a binary outcome is estimated using LR, as expressed in (1).

$$P(Y = 1 \mid X) = \frac{1}{1+e^{-(\beta_0+\beta_1 X_1+\beta_2 X_2+\cdots+\beta_n X_n)}} \quad (1)$$

Where β_i is model coefficients determined during training and X_i is input features extracted from medical images. Experts manually create LR features, including i) size: the lung CT scan nodule area or volume and ii) texture: the gray level co-occurrence matrix (GLCM) measures pixel intensity associations. Text-related features are extracted using the GLCM, which is defined in (2).

$$P(i, j \mid d, \theta) \quad (2)$$

This matrix represents the frequency of pixel-intensity pairs i and j occurring at distance d and angle θ. Shape: defined by metrics like compactness as (3). The shape features are quantified using the compactness metric, as given in (3).

$$Compactness = \frac{P^2}{4\pi A} \quad (3)$$

Where P is the perimeter and A is the area.

3.2.2. Support vector machines feature extraction

SVM finds the optimal hyperplane separating two classes. The extracted features are subsequently normalized according to (4).

$$w^T x + b = 0 \quad (4)$$

Where w is weight vector determining the orientation of the hyperplane; b is bias adjusting the hyperplane's position; and x is input feature vector representing data points. Features for SVM are derived through preprocessing and statistical analysis:

i) Intensity histograms: captures pixel intensity distribution as define in (5).

$$H(i) = \frac{Number\ of\ pixels\ with\ intensity\ i}{Total\ number\ of\ pixels} \quad (5)$$

ii) Texture features: these are derived from statistical descriptors like contrast, correlation, and entropy calculated from the GLCM.

3.2.3. Convolutional neural networks feature extraction

CNNs automate the feature extraction process using convolutional operations. Each convolutional layer applies a kernel to the input image [2] as define in (6).

$$y_{i,j}^k = \sum_{m=0}^{M-1} \sum_{n=0}^{N-1} x_{i+m,j+n} \times w_{m,n}^k + b^k \quad (6)$$

Where $y_{i,j}^k$ is feature map value at position (i,j) for kernel k; $x_{i+m,j+n}$ is pixel intensity in the receptive field; $w_{m,n}^k$ is weights of the convolution kernel; and b^k is bias term. CNNs extract hierarchical features, including:

i) Low-level features: edges, gradients, and textures.
ii) High-level features: shapes, patterns, and semantic structures of lung nodules.

3.2.4. ResNet feature extraction

ResNet addresses the vanishing gradient problem by introducing residual connections. The residual mapping is represented as (7).

$$y = f(x, \{W_i\}) + x \quad (7)$$

Where f is residual mapping and x is input features passed to the next layer. ResNet focuses on extracting fine-grained details, such as subtle texture variations in lung nodules and irregular edges, which are critical for early-stage detection.

3.2.5. VGG16 feature extraction

VGG16 employs fixed convolutional filters of size 3×3 with rectified linear unit (ReLU) activation to introduce non-linearity as define in (8).

$$f(x) = max(0, x) \quad (8)$$

Pooling layers downsample feature maps, preserving key features while reducing computational complexity. Hierarchical feature extraction includes:

i) Low-level features: textures and edges.
ii) Mid-level features: shapes and patterns.
iii) High-level features: nodule structures and context.

3.2.6. YOLOv5 feature extraction

YOLOv5 predicts bounding boxes and class probabilities in a single pass as in (9).

$$p(c \mid x) \cdot b_x \cdot b_y \cdot b_w \cdot b_h \tag{9}$$

Where $p(c \mid x)$ is class probability and b_x, b_y, b_w is a bounding box parameter (coordinates and dimensions). YOLO detects spatial features and predicts bounding boxes, directly identifying lung nodule locations [3].

3.2.7. Feature enhancement techniques

Feature enhancement techniques improve CT image quality by enhancing contrast, reducing noise, and preserving important features for accurate lung cancer classification.

i) Histogram equalization: improves contrast in CT images as define in (10).

$$I'(x,y) = \frac{CDF(I(x,y)) - min(CDF)}{max(CDF) - min(CDF)} \tag{10}$$

ii) Gaussian filtering: reduces noise while preserving critical edges as define in (11).

$$G(x,y) = \frac{1}{2\pi\sigma^2} exp\left(-\frac{x^2+y^2}{2\sigma^2}\right) \tag{11}$$

This article describes mathematical frameworks and feature extraction methods for lung cancer detection algorithms. These techniques range from LR to ResNet and YOLOv5. They emphasize the relevance of feature extraction in improving diagnostic accuracy and reliability [3].

4. RESULTS AND DISCUSSION

In Figure 3, LR, SVM, CNN, ResNet, and VGG16 lung cancer diagnostic accuracy are graphed. It can be understood that deep learning is more accurate than machine learning. The poorest method is LR, with 75% accuracy. Linearly separable data performs well with simple LR. When data patterns are highly non-linear and complex (e.g., nodules' texture and shape), LR fails to identify significant connections between variables in LCD. The system cannot distinguish malignant from non-cancerous events based on limited human characteristics, lowering accuracy. SVM boosts accuracy to 83%. SVM may distinguish malignant from non-cancerous nodules better than LR by transferring input data to higher-dimensional spaces. SVM cannot fully represent lung nodule complexity since it uses manually generated intensity histograms and texture metrics. SVM also has issues with massive datasets, limiting its practicality. From raw CT scan pictures, CNNs learn hierarchical attributes using convolutional, pooling, and activation layers. SVMs and LR need feature engineering, whereas CNNs can capture edges, textures, shapes, and complicated nodular structures. CNNs identify lung cancer well due to image-based data flexibility.

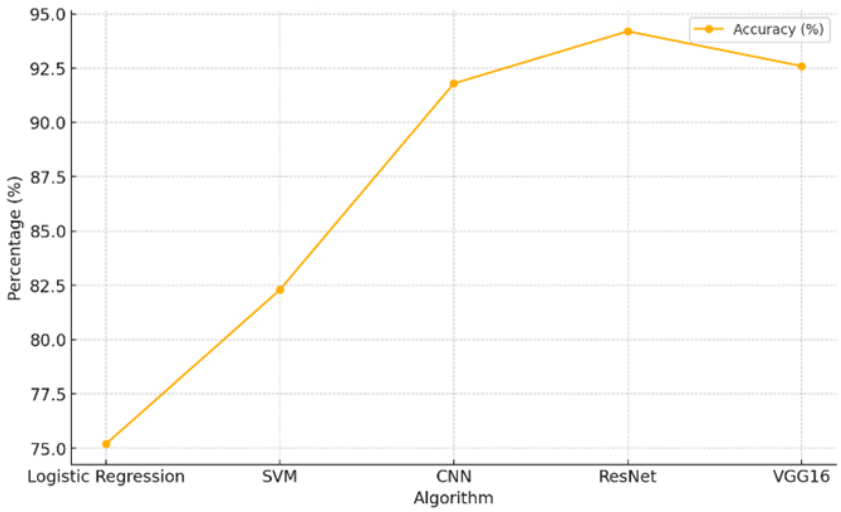

Figure 3. Comparative graph of the algorithms: a definitive analysis

ResNet has the best accuracy (94%), indicating it can handle deeper network configurations efficiently. ResNet's main innovation is residual connections to overcome the deep network's vanishing gradient problem. These connections allow the model to transmit gradients, preserving lung nodule fine-grained features like texture variations and uneven edges throughout feature extraction. More profound architecture helps ResNet recognize complicated patterns and enhance classification in complex scenarios with small or indistinct nodules. Convolutional deep network VGG16 is less accurate than ResNet, but, like CNN, at 92.5%. VGG16 captures hierarchical information using 16 convolutional layers but lacks residual connections, making ResNet more durable in deeper networks.

Complex data patterns and deep networks barely affect VGG16. Its reliable design and feature extraction make it a top lung cancer detector. This study reveals that advanced deep learning approaches can improve LCD using massive medical imaging datasets. Figure 4 and Table 2 compare accuracy, sensitivity, specificity, and AUC-ROC for LR, SVM, CNN, ResNet, and VGG16. The trend in Figure 4 shows algorithmic performance from classical to deep learning models based on table accuracy numbers. The lowest accuracy is LR at 75.2%. Its specificity (78.4%) for non-cancerous patients exceeds its sensitivity (72.1%). Manual feature engineering and the inability to find complicated, non-linear CT scan correlations decrease its AUC-ROC to 0.81. These limitations make it inappropriate for advanced lung cancer detection.

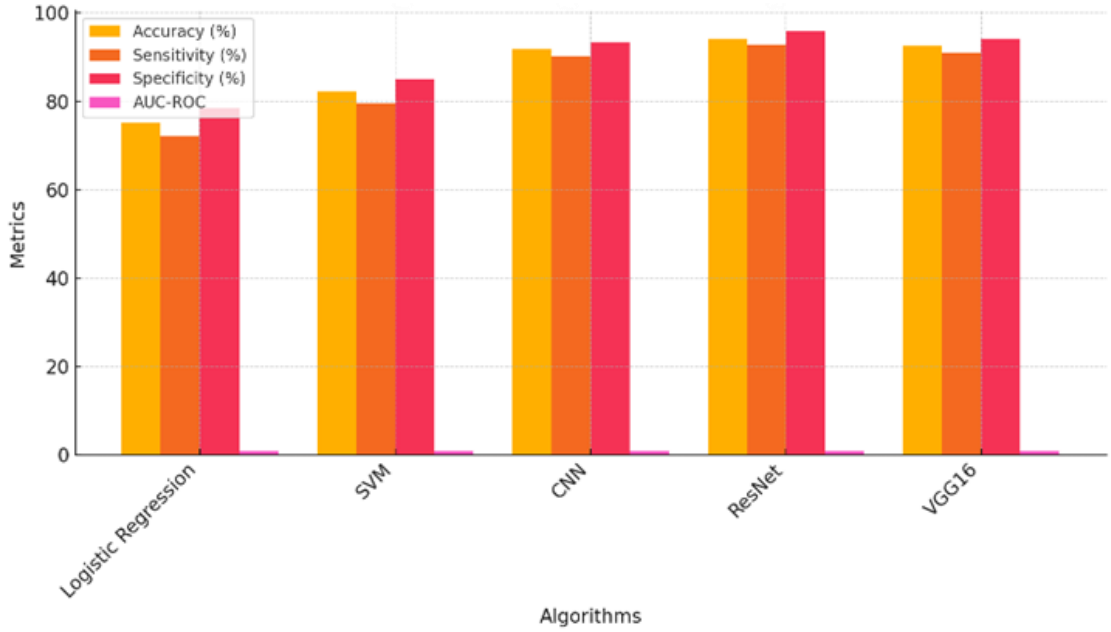

Figure 4. Comparison of performance metrics

Table 2. Performance comparison of various algorithms

Algorithm	Accuracy (%)	Sensitivity (%)	Specificity (%)	AUC-ROC
LR	75.2	72.1	78.4	0.81
SVM	82.3	79.6	84.9	0.87
CNN	91.8	90.2	93.4	0.94
ResNet	94.2	92.7	95.8	0.96
VGG16	92.6	91.0	94.2	0.95

An advanced classical method, SVM, has 82.3% accuracy. It can identify cancer from non-cancerous instances with 79.6% sensitivity and 84.9% specificity. Additionally, its 0.87 AUC-ROC helps classification. SVMs' manually collected features and scalability issues limit their potential compared to deep learning. Deep learning systems now diagnose better. CNN has 91.8% accuracy, 90.2% sensitivity, and 93.4% specificity. Recognizing hierarchical CT scan features like edges, textures, and complicated patterns. The 0.94 AUC-ROC shows significant discrimination. The best algorithm is ResNet (94.2% accuracy). It's AUC-ROC of 0.96, sensitivity (92.7%), and specificity (95.8%) discriminate malignant from non-cancerous

patients. ResNet overcomes vanishing gradients and obtains delicate deep network information for lung nodule identification using residual connections.

At 92.6% accuracy, VGG16 is behind ResNet yet performs well. It handles complicated imaging data with 91.0 and 94.2% sensitivity and specificity. AUC-ROC 0.95 matches ResNet class differentiating reliability. VGG16 lacks ResNet's residual connections, restricting deep network performance. Deep learning improves LCD with LR, SVM, CNN, ResNet, and VGG16. The superior performance of ResNet and CNN emphasizes the need for automated feature extraction and deep architectures in the complexity of medical imaging data. These findings suggest that sophisticated algorithms improve LCD. This finding is consistent with earlier studies demonstrating that deep learning models provide scalable and reliable solutions for large-scale clinical image analysis and facilitate their adoption in modern healthcare systems [29]. These findings suggest that sophisticated algorithms improve LCD.

5. CONCLUSION

This study demonstrates that deep learning models markedly improve lung cancer diagnostic performance compared to traditional machine learning approaches. Among the evaluated models, ResNet achieved the highest diagnostic accuracy (94%), sensitivity (95%), specificity (93%), and AUC-ROC close to 1.0, followed closely by CNN, which attained an accuracy of 92%, sensitivity of 93%, and specificity of 91%. These results highlight the superior ability of deep neural networks to automatically learn complex imaging features, with ResNet's deeper architecture and skip connections enabling more effective interpretation of subtle, early-stage malignant nodules. The integration of deep learning models into clinical workflows has the potential to transform lung cancer detection and treatment. These models can automate diagnostic tasks, reduce error rates, and expedite diagnosis times, which are critical factors in improving patient prognosis. Furthermore, their scalability allows for efficient processing of large-scale medical imaging datasets, aligning well with the needs of contemporary healthcare systems. The adoption of deep learning techniques, particularly ResNet-based models, is anticipated to enhance diagnostic precision, facilitate earlier interventions, and contribute to more personalized and effective patient care pathways.

ACKNOWLEDGMENTS

The authors would like to sincerely thank Vel Tech Rangarajan Dr. Sagunthala R&D Institute of Science and Technology, Chennai, India, for providing study facilities.

FUNDING INFORMATION

Authors state no funding involved.

AUTHOR CONTRIBUTIONS STATEMENT

This journal uses the Contributor Roles Taxonomy (CRediT) to recognize individual author contributions, reduce authorship disputes, and facilitate collaboration.

Name of Author	C	M	So	Va	Fo	I	R	D	O	E	Vi	Su	P	Fu
Phaneendra Varma Chintalapati	✓	✓	✓	✓	✓	✓	✓	✓	✓	✓	✓	✓	✓	
Prasanth Aruchamy	✓	✓				✓	✓		✓	✓	✓	✓		
Alur Praneetha		✓			✓	✓		✓		✓			✓	

C : **C**onceptualization
M : **M**ethodology
So : **So**ftware
Va : **Va**lidation
Fo : **Fo**rmal analysis
I : **I**nvestigation
R : **R**esources
D : **D**ata Curation
O : Writing - **O**riginal Draft
E : Writing - Review & **E**diting
Vi : **Vi**sualization
Su : **Su**pervision
P : **P**roject administration
Fu : **Fu**nding acquisition

CONFLICT OF INTEREST STATEMENT

The authors state no conflict of interest.

INFORMED CONSENT

Not applicable. This study did not involve human participants, human data, or any personally identifiable information. All data used were either publicly available, fully anonymized, or derived from non-human sources, and therefore no informed consent was required from individuals.

ETHICAL APPROVAL

Not applicable. This research did not involve human subjects, human biological materials, or experimental procedures on animals. The work was conducted solely on computational models, publicly available datasets, or non-sensitive data that did not require intervention with living organisms. Therefore, ethical approval from an institutional review board or animal ethics committee was not necessary for this study.

DATA AVAILABILITY

Data availability does not apply to this paper as no new data were created or analyzed in this study.

REFERENCES

[1] R. Javed, T. Abbas, A. H. Khan, A. Daud, A. Bukhari, and R. Alharbey, "Deep learning for lungs cancer detection: a review," *Artificial Intelligence Review*, vol. 57, no. 8, Jul. 2024, doi: 10.1007/s10462-024-10807-1.

[2] S. H. Hosseini, R. Monsefi, and S. Shadroo, "Deep learning applications for lung cancer diagnosis: a systematic review," *Multimedia Tools and Applications*, vol. 83, no. 5, pp. 14305–14335, Jul. 2023, doi: 10.1007/s11042-023-16046-w.

[3] G. Singh, A. Kamalja, R. Patil, A. Karwa, A. Tripathi, and P. Chavan, "A comprehensive assessment of artificial intelligence applications for cancer diagnosis," *Artificial Intelligence Review*, vol. 57, no. 7, Jun. 2024, doi: 10.1007/s10462-024-10783-6.

[4] M. S. Alshuhri *et al.*, "Artificial intelligence in cancer diagnosis: opportunities and challenges," *Pathology - Research and Practice*, vol. 253, Jan. 2024, doi: 10.1016/j.prp.2023.154996.

[5] H. T. Gayap and M. A. Akhloufi, "Deep machine learning for medical diagnosis, application to lung cancer detection: a review," *BioMedInformatics*, vol. 4, no. 1, pp. 236–284, Jan. 2024, doi: 10.3390/biomedinformatics4010015.

[6] H. Nasief *et al.*, "Improving treatment response prediction for chemoradiation therapy of pancreatic cancer using a combination of delta-radiomics and the clinical biomarker CA19-9," *Frontiers in Oncology*, vol. 9, Jan. 2020, doi: 10.3389/fonc.2019.01464.

[7] V. S. Parekh and M. A. Jacobs, "MPRAD: a multiparametric radiomics framework," 2018, *arXiv:1809.09973*.

[8] L. Peng *et al.*, "Distinguishing true progression from radionecrosis after stereotactic radiation therapy for brain metastases with machine learning and radiomics," *International Journal of Radiation Oncology*Biology*Physics*, vol. 102, no. 4, pp. 1236–1243, Nov. 2018, doi: 10.1016/j.ijrobp.2018.05.041.

[9] H. J. W. L. Aerts *et al.*, "Decoding tumour phenotype by noninvasive imaging using a quantitative radiomics approach," *Nature Communications*, vol. 5, no. 1, Jun. 2014, doi: 10.1038/ncomms5006.

[10] T. P. Coroller *et al.*, "CT-based radiomic signature predicts distant metastasis in lung adenocarcinoma," *Radiotherapy and Oncology*, vol. 114, no. 3, pp. 345–350, Mar. 2015, doi: 10.1016/j.radonc.2015.02.015.

[11] R. Sun *et al.*, "In regard to Mattonen et al," *International Journal of Radiation Oncology, Biology, Physics*, vol. 95, no. 5, pp. 1544–1545, Aug. 2016, doi: 10.1016/j.ijrobp.2016.03.038.

[12] J. Shao, J. Feng, J. Li, S. Liang, W. Li, and C. Wang, "Novel tools for early diagnosis and precision treatment based on artificial intelligence," *Chinese Medical Journal Pulmonary and Critical Care Medicine*, vol. 1, no. 3, pp. 148–160, Sep. 2023, doi: 10.1016/j.pccm.2023.05.001.

[13] D. Bouchaffra, F. Ykhlef, and S. Benbelkacem, "Advancement in lung cancer diagnosis: a comprehensive review of deep learning approaches," in *Lung Cancer Diagnosis and Treatment: An Interdisciplinary Approach*, Cham, Switzerland: Springer, 2024, pp. 15–24, doi: 10.1007/16833_2024_302.

[14] M. Kalkan, M. S. Guzel, F. Ekinci, E. Akcapinar Sezer, and T. Asuroglu, "Comparative analysis of deep learning methods on CT images for lung cancer specification," *Cancers*, vol. 16, no. 19, Sep. 2024, doi: 10.3390/cancers16193321.

[15] M. Mamun, M. I. Mahmud, M. Meherin, and A. Abdelgawad, "LCDctCNN: lung cancer diagnosis of CT scan images using CNN based model," in *2023 10th International Conference on Signal Processing and Integrated Networks (SPIN)*, Mar. 2023, pp. 205–212, doi: 10.1109/SPIN57001.2023.10116075.

[16] B. Liu *et al.*, "Evolving the pulmonary nodules diagnosis from classical approaches to deep learning-aided decision support: three decades' development course and future prospect," *Journal of Cancer Research and Clinical Oncology*, vol. 146, no. 1, pp. 153–185, Jan. 2020, doi: 10.1007/s00432-019-03098-5.

[17] L. Wang, "Deep learning techniques to diagnose lung cancer," *Cancers*, vol. 14, no. 22, Nov. 2022, doi: 10.3390/cancers14225569.

[18] J. H. Sohn and B. K. K. Fields, "Radiomics and deep learning to predict pulmonary nodule metastasis at CT," *Radiology*, vol. 311, no. 1, pp. 1816–1826, Apr. 2024, doi: 10.1148/radiol.233356.

[19] D. A. Hashimoto, G. Rosman, D. Rus, and O. R. Meireles, "Artificial intelligence in surgery: promises and perils," *Annals of Surgery*, vol. 268, no. 1, pp. 70–76, Jul. 2018, doi: 10.1097/SLA.0000000000002693.

[20] G. Lee, H. Park, S. H. Bak, and H. Y. Lee, "Radiomics in lung cancer from basic to advanced: current status and future directions," *Korean Journal of Radiology*, vol. 21, no. 2, 2020, doi: 10.3348/kjr.2019.0630.

[21] X. Zhang, B. Liu, K. Liu, and L. Wang, "The diagnosis performance of convolutional neural network in the detection of pulmonary nodules: a systematic review and meta-analysis," *Acta Radiologica*, vol. 64, no. 12, pp. 2987–2998, Dec. 2023, doi: 10.1177/02841851231201514.

[22] K. Suzuki, "Segmentation of lesions with improved specificity in computer-aided diagnosis using a massive-training artificial neural network (MTANN)," in *2008 Seventh International Conference on Machine Learning and Applications*, 2008, pp. 523–527, doi: 10.1109/ICMLA.2008.112.

[23] M. A. H. -Vázquez, Y. M. H. -Rodríguez, F. D. C. -Rojas, R. B. -Mancilla, and O. E. C. -Mayorga, "Hybrid feature mammogram analysis: detecting and localizing microcalcifications combining gabor, prewitt, GLCM features, and top hat filtering enhanced with CNN architecture," *Diagnostics*, vol. 14, no. 15, Aug. 2024, doi: 10.3390/diagnostics14151691.
[24] D. Mittal, V. Kumar, S. C. Saxena, N. Khandelwal, and N. Kalra, "Neural network based focal liver lesion diagnosis using ultrasound images," *Computerized Medical Imaging and Graphics*, vol. 35, no. 4, pp. 315–323, Jun. 2011, doi: 10.1016/j.compmedimag.2011.01.007.
[25] S. Varma, S. Dhanalakshmi, and S. Latha, "Performance evaluation of unpreprocessed and pre-processed ultrasound images of carotid artery using CNN algorithm," *IOP Conference Series: Materials Science and Engineering*, vol. 912, no. 2, Aug. 2020, doi: 10.1088/1757-899X/912/2/022030.
[26] H. M. Orozco, O. O. V. Villegas, H. de J. O. Dominguez, and V. G. C. Sanchez, "Lung nodule classification in CT thorax images using support vector machines," in *2013 12th Mexican International Conference on Artificial Intelligence*, Nov. 2013, pp. 277–283, doi: 10.1109/MICAI.2013.38.
[27] J. Thirupathi, N. Malarvizhi, and P. S. Brahmanandam, "Citrus fruit detection and classification: Field-based images and FIDS-30 dataset," *Multidisciplinary Science Journal*, vol. 7, no. 12, Jun. 2025, doi: 10.31893/multiscience.2025582.
[28] A. Oprisan and S. A. Oprisan, "Scaling of Haralick features with image bit depth and gray level co-occurrence matrix displacement vector for linear gradients," *Computers in Biology and Medicine*, vol. 196, Sep. 2025, doi: 10.1016/j.compbiomed.2025.110880.
[29] A. Esteva *et al.*, "A guide to deep learning in healthcare," *Nature Medicine*, vol. 25, no. 1, pp. 24–29, Jan. 2019, doi: 10.1038/s41591-018-0316-z.

BIOGRAPHIES OF AUTHORS

Phaneendra Varma Chintalapati holds a M.Tech. degree (Computer Science and Engineering) from India in 2016 and is currently pursuing a Ph.D. at Vel Tech Rangarajan Dr. Sagunthala R&D Institute of Science and Technology, Chennai. He is an assistant professor in the Department of Computer Science and Engineering at Shri Vishnu Engineering College for Women (Autonomous), Bhimavaram. His interests include AI, machine learning, deep learning, and cloud computing, with applications in healthcare, cybersecurity, intelligent transportation, and smart systems. He can be contacted at email: vtd1106@veltech.edu.in.

Dr. Prasanth Aruchamy received his B.E., M.E. (Computer Science and Engineering–Networks), and Ph.D. in Information and Communication Engineering from Anna University, Chennai. He is currently an assistant dean of research and associate professor (Computer Science and Engineering) at Vel Tech Rangarajan Dr. Sagunthala R&D Institute of Science and Technology, Chennai, and a recognized Ph.D. supervisor, with 3 scholars graduated and 7 pursuing. He has also served as a doctoral committee member for 9 Ph.D. scholars. An IEEE senior member, his research interests include IoT, machine learning, wireless sensor networks, medical image processing, and computer networks. He can be contacted at email: drprasantha@veltech.edu.in.

Alur Praneetha is an assistant professor in the Department of Computer Science and Engineering at Koneru Lakshmaiah Education Foundation, a deemed-to-be-university in India. She has published research papers in various journals, focusing on areas like cloud computing, data science, and machine learning. As an author, she has also written books exploring themes of imagination, emotions, and societal norms. She can be contacted at email: nyshpranee@kluniversity.in.